Research Article ISSN 2641-4333

Neurology - Research & Surgery

Multimodal EEG Biomarkers of Cognitive Decline: BrainView-Based Detection of Early Alzheimer's Disease

Annie TL Young, Ph.D[1], Slav Danev[2], Jonathan RT Lakey, Ph.D, MSM[1]*

[1]*Department of Surgery and Biomedical Engineering, University of California Irvine, California, USA.*

[2]*Medeia Inc, Santa Barbara, CA, USA.*

***Correspondence:**
Jonathan RT Lakey, PhD, MSM, Department of Surgery, 333 City Blvd West, Suite 1600, Orange, California, USA, Phone: 1-949-824-8022, Fax: 1-714-456-6188.

Received: 02 Sep 2025; **Accepted:** 17 Oct 2025; **Published:** 25 Oct 2025

Citation: Annie TL Young, Slav Danev, Jonathan RT Lakey. Multimodal EEG Biomarkers of Cognitive Decline: BrainView-Based Detection of Early Alzheimer's Disease. Neurol Res Surg. 2025; 8(4): 1-17.

ABSTRACT

Background: *Early detection of Alzheimer's disease (AD) is critical for timely intervention, yet current diagnostic tools can be costly and invasive. Quantitative electroencephalography (qEEG) and event-related potentials (ERPs) offer non-invasive, cost-effective alternatives with high temporal resolution.*

Objective: *This study evaluated the BrainView system, a multi-modal EEG platform integrating qEEG, source localization, ERP analysis, and machine learning, to assess its utility in detecting early cognitive decline.*

Methods: *Z-scored brain maps, sLORETA source localization, and ERP waveforms were analyzed in individuals with suspected early AD. Key frequency ratios and cortical activity patterns were compared against normative databases. Machine learning models, including XGBoost with LASSO regression, were trained to classify cognitive status.*

Results: *Elevated delta and theta activity, alongside reduced alpha and beta power, reflected typical EEG slowing associated with early AD. sLORETA localized these abnormalities to frontal and parietal regions. ERP analysis revealed attenuated P200 responses and atypically early, amplified P300 components, suggesting possible compensatory mechanisms. The XGBoost machine learning model achieved high classification accuracy (sensitivity = 0.88, specificity = 0.94), supporting the diagnostic value of EEG-based features.*

Conclusion: *The BrainView system effectively identifies neurophysiological patterns consistent with early AD. Combined with machine learning, EEG-based tools offer a scalable, non-invasive approach for early cognitive screening and monitoring. Further validation in larger, diverse cohorts is needed to support clinical integration.*

Keywords

BrainView, qEEG, Event-related potentials, ERP, Evoked potentials, Alzheimer's Disease, Mild cognitive impairment, sLORETA, Brain mapping, z-score power, Frequency bands.

Introduction

Alzheimer's disease (AD) is the most common form of dementia, accounting for approximately 60–80% of cases worldwide [1,2]. While it primarily affects individuals over the age of 65, early-onset cases in younger populations are also observed [3,4]. Currently, over 55 million people globally are living with dementia, and this number is projected to rise to 130–140 million by 2050, with AD comprising the majority of cases [5-7].

AD is a progressive neurodegenerative disorder characterized by memory loss, cognitive decline, behavioral disturbances, and eventual loss of functional independence [8,9]. Pathologically, AD is defined by the accumulation of amyloid-β plaques and

hyperphosphorylated tau tangles, which disrupt synaptic function, contribute to neuronal hyperexcitability, and impair network dynamics [10-12]. Functional disruptions are especially prominent in core brain networks such as the default mode network (DMN), and abnormal neuronal oscillations are frequently observed [13-16]. Additionally, mitochondrial dysfunction, oxidative stress, and chronic neuroinflammation have emerged as key contributors to AD pathophysiology [10,11,17,18].

The global burden of AD is immense, both personally and economically. In 2023, the estimated cost of dementia care exceeded $1.3 trillion [19]. Current treatments offer only symptomatic relief and do not halt or reverse disease progression [20]. Thus, early detection is critical, particularly at the stage of amnestic mild cognitive impairment (aMCI), which frequently precedes AD [10,20-23]. A substantial proportion of aMCI patients convert to AD, although some remain stable or even revert to normal cognition [24]. Therefore, accurate risk prediction at the MCI stage is vital for enabling timely, individualized intervention.

Despite the promise of biomarker-based diagnostics (e.g., MRI, PET imaging, and cerebrospinal fluid (CSF) analysis), these methods are often costly, invasive, and inaccessible, particularly in low-resource settings [21,25-30]. This has spurred interest in alternative diagnostic approaches that are less invasive, more affordable, and scalable. Electroencephalography (EEG), particularly quantitative EEG (qEEG) and event-related potentials (ERPs), offers such potential [31,32]. EEG is low-cost, non-invasive, and provides high temporal resolution, making it ideal for detecting subtle functional brain changes before structural abnormalities become evident. Resting-state EEG, in particular, is well-tolerated by patients and has been shown to reveal distinct differences between healthy aging, MCI, and AD [21,33-42].

Typical EEG abnormalities in AD include increased low-frequency (delta, theta) activity, reduced high-frequency (alpha, beta, gamma) activity, decreased signal complexity, and disrupted neural synchronization [37,39,42-50]. These changes reflect slower brain electrical activity and reduced network efficiency, hallmarks of neurodegeneration.

ERPs provide complementary information, especially in cognitive paradigms like the auditory oddball task [51,52]. In AD, P300 components (P3a and P3b) are typically reduced in amplitude and delayed in latency, indicating deficits in attention, stimulus discrimination, and cognitive updating [22,53-59]. These ERP changes correlate with behavioral impairments such as slower reaction times and reduced accuracy, and have shown predictive value for MCI-to-AD progression [60-62]. However, ERP adoption in clinical practice remains limited due to technical and standardization challenges [60,63-66].

In this study, we evaluate the diagnostic potential of the BrainView system (developed by Medeia Inc.), which integrates resting-state EEG, ERP data, neuropsychological assessments, and a machine learning classifier (XGBoost). This prototype diagnostic classifier is developed using novel metrics derived from resting-state EEG and ERPs to assess brain activity. Our primary objective is to identify the EEG and ERP features that best discriminate AD patients from non-AD controls. The **secondary objective** is to identify features that reflect disease staging and differentiate AD from other dementia types. This proof-of-concept study aims to demonstrate the utility of the BrainView system as a rapid, accessible, and objective tool for early detection of pathological brain aging. Notably, the BrainView model has achieved a sensitivity of 0.88 and a specificity of 0.94 in distinguishing individuals with AD from non-AD control ─ performance metrics that underscore its potential clinical utility as a reliable screening tool. These results suggest that the model can accurately identify true positive cases while minimizing false positives, making it well-suited for early detection and risk stratification in diverse clinical settings. Ultimately, this approach may support more informed and data-driven decision-making in the diagnosis, monitoring, and management of AD.

Materials and Methods

A. *Subject and Variable Selection*

Patient data were collected between 2018 and 2024 across multiple neurology clinics. The present data were collected as part of a seven-site multicentre clinical trial focused on discriminating patients with AD from normal healthy older adults. As part of the trial protocol, both event-related ERPs and resting-state EEG data were obtained, in addition to a comprehensive neuropsychological battery.

The dataset includes two groups: **83 patients diagnosed with mild AD** and a **control group of 2,000 non-AD individuals ('healthy')**, with the primary aim of distinguishing AD patients from controls. Participants were between **55 and 85 years old**, with **52% identifying as female**. Each participant underwent a comprehensive evaluation that included:

- A **full neuropsychological assessment battery** commonly used in AD evaluations
- **Resting-state EEG** recorded from 19 channels (5 minutes with eyes open, 5 minutes with eyes closed)
- **ERPs** using an **oddball paradigm**, which included:
  - Standard tones: 1000 Hz (probability = 0.75)
  - Target tones: 2000 Hz (probability = 0.15)
  - Distractor tones: White noise (probability = 0.10)
  - A total of 100–200 stimuli, presented binaurally at 70 dB

This multimodal data collection was designed to capture both spontaneous and task-related brain activity, facilitating more accurate classification of early-stage AD.

Resting EEG samples, obtained with eyes closed or open and free from artifacts, underwent analysis. Fast-Fourier Transformation (FFT) and direct Fourier Transform (Complex Demodulation) techniques were applied to extract at the spectral power resolution of 0.5 Hz the five primary frequency bands [Delta (0–4Hz), Theta (4–8Hz), Alpha (8–12Hz), Beta (low: 13-21; high: 21-35 Hz), and Gamma (35-45Hz)] and the standard ratios of frequency bands.

Statistical analyses included generation of topographical color maps for 19 monopolar and all 171 possible combinations of the 19 electrode bipolar derivations of the EEG [67].

Delta Waves: This type of brain wave has the highest amplitude and occurs at the slowest frequency. It is primarily observed during deep sleep.

Theta Waves: These brain waves are present when awake or in a light phase of sleep, such as when falling asleep. When occurring while awake, theta waves are associated with intense relaxation and are believed to play a crucial role in information processing and memory formation.

Alpha Waves: Produced when awake but in a very relaxed state, typically experienced when first waking up and not concentrating on anything specific.

Beta Waves: These brain waves are generated when the brain is fully awake, alert, and focused. They also occur during states of excitement or arousal.

Gamma Waves: Waves with the lowest amplitude but the fastest frequency among brain waves. They are generated when an individual is trying to solve a problem or intensely concentrating on a specific task, such as during learning.

B. *Inclusion/Exclusion Criteria, Demographics and Gender*

Subjects completed a neurological history questionnaire for them, and psychometric evaluations were conducted. Adults (≥ 18 years) also completed a neurological questionnaire, and those deemed unhealthy were excluded based on questionnaire responses and/or physician comments. Physicians have access to the following questionnaires: GAD-7 (Anxiety Severity), DSM-5 Level 1 (Cross-Cutting Symptom Measures), PHQ-9 (Depression), PCL-C (PTSD Severity), and general neurological questionnaires. Inclusion required at least one questionnaire score below moderate and physician-verified health in that the patient was deemed healthy. Any patient records or previously known medical records with questionnaire score of 'moderate' or 'severe' were excluded from the BrainView EEG database, regardless of other information.

C. *Demographic Characteristics*

It is crucial that the demographic mixture of males and females, various ethnic groups, and socioeconomic statuses be reasonably representative of the expected North American clientele. This diversity was derived from a large pool of subjects obtained from eight geographically dispersed sites, reflecting the North American demographics and addressing a wide range of ethnic and socioeconomic statuses found in the de-identified patient data before review.

D. *Client-Based BrainView qEEG Database*

Each client in the BrainView qEEG database completed a DSM-based questionnaire. Regression analysis was utilized to remove any psychopathology-related variance from the EEG data. This process ensures that the variance in the EEG of 'healthy' subjects, which is explained by the variance in the questionnaire, is removed to create a 'psychopathology-free' qEEG normative database or discriminant databases for various brain disorders.

Utilizing a client-based normative or discriminant database has its own set of advantages. Clients may harbor expectations distinct from those of 'healthy' subjects concerning EEG recordings. Given that it is common for clients to experience worry or stress during EEG sessions, research has demonstrated a significant correlation between anxiety levels and the power distribution of the frequency band spectrum [68,69]. In essence, profound differences may exist in the resting state EEG recordings of clients compared to 'healthy' subjects, differences unrelated to the psychological complaints of the clients. Therefore, comparing a client's EEG with a normative database comprising 'healthy' subjects without accounting for the aforementioned variations might lead to incorrect conclusions and render the treatment ineffective.

E. *Discriminant Databases for Various Brain Disorders*

In discriminant databases using quantitative EEG (qEEG), identifying the most effective discriminant functions is challenging due to three key issues [70]:

1. The wide range of possible analytic methods and features (e.g., time-domain, frequency-domain, and hybrid time-frequency measures).
2. The need for high specificity in distinguishing between similar conditions (e.g., mild traumatic brain injury vs. fatigue).
3. The reliance on individualized baselines or "ground truth" for accurate comparisons, which is often unavailable in real-world scenarios.

Discriminant functions are models used to classify data into specific groups based on qEEG features. Machine learning, particularly when supported by platforms like Medeia Inc.'s BrainView, enables automated pattern recognition in qEEG data. These models require domain expertise for effective feature selection, which is essential for accurate classification and outlier detection. Rule-based learning helps make these models interpretable by identifying key decision rules derived from the data.

For data analysis, AD patients were compared to cognitively 'healthy' (non-AD) controls using both LASSO logistic regression and the XGBoost (Extreme Gradient Boosting) classifier. XGBoost is a high-performance gradient boosting algorithm that constructs models by sequentially adding decision trees, with each tree aiming to correct the errors of the previous one [71]. This method offers an optimal balance between predictive accuracy and computational efficiency, making it particularly suitable for clinical prediction tasks.

One key advantage of XGBoost is its ability to generate feature importance scores, allowing researchers to identify which variables, such as neuropsychological test results or depressive symptom indicators, most strongly influence the model's predictions, thus providing clinically meaningful insights [71]. Compared to other

machine learning models such as Random Forest, AdaBoost, Bagging, and Naive Bayes, the XGBoost framework, particularly when combined with SHAP (SHapley Additive exPlanations), demonstrates [72]:

- Higher classification accuracy,
- Greater sensitivity in detecting minority classes, and
- Improved interpretability of complex predictive relationships.

F. *Low-Resolution Brain Electromagnetic Tomography*

Another important set of metrics from BrainView is derived through **source analysis**, an advanced EEG technique that localizes brain electrical activity by solving the *inverse problem*, translating scalp-recorded potentials into estimates of their neural origins. A key method used is **LORETA** (Low-Resolution Brain Electromagnetic Tomography), which generates a three-dimensional distribution of neuronal activity within the brain's grey matter based on surface EEG data [73].

LORETA allows researchers to trace which brain regions are active during specific tasks or mental states, offering insights into both spatial and temporal dynamics of neural processing. It is compatible with various EEG systems and does not rely on fixed electrode setups. Quantitative LORETA compares a patient's brain activity to a normative database (40,000+ subjects) to assist in diagnosis, treatment monitoring, and clinical decision-making. It produces 3D brain maps for interpreting functional brain states with greater precision.

Results

A. *Z-Scored Power Brain Map – Waveform Ratios*

Z-scored brain mapping is a powerful tool used to visualize deviations from 'healthy' EEG patterns. By expressing differences in brainwave activity as standard deviations (SD) from normative data, it becomes easier to detect abnormalities that may be associated with cognitive impairment. This approach is especially valuable in applications such as dementia screening, neurofeedback, and qEEG-based diagnostics.

Figures 1 and 2 present z-scored brain maps, which highlight how the relative power in various EEG frequency bands differs from a 'healthy' population average. In these maps:

- A **z-score of 0 SD** indicates activity consistent with a 'healthy' norm.
- **Positive z-scores** (+1 to +3 SD) reflect **increased activity** in a frequency band.
- **Negative z-scores** (–1 to –3 SD) indicate **decreased activity**.

In Figure 1, the qEEG brain maps show **notable increases in slow-wave activity**, particularly across ratios involving theta and delta frequencies. Several key ratios — **theta/alpha, theta/beta, delta/alpha, and delta/beta** — are highly elevated, appearing in the red-to-orange range of the z-score color scale. These correspond to z-scores between **+2 and +3 SD**, indicating that slow-frequency brainwaves (theta and delta) are dominating over faster ones (alpha and beta). This is a hallmark of **EEG slowing**, commonly associated with **AD** and **MCI**. Specifically:

- The **theta/alpha ratio** is elevated with z-scores around **+2.5 to +3 SD**, reflecting significantly higher theta power relative to alpha.
- The **theta/beta ratio** shows a similar elevation, reinforcing the pattern of slow-wave dominance.
- The **delta/alpha and delta/beta ratios** are also strongly elevated (up to **+3 SD**), indicating increased delta activity in relation to faster frequencies.
- The **theta/high beta** and **delta/high beta** ratios are elevated but to a slightly lesser extent (approximately **+2 to +2.5 SD**).

Conversely, the **delta/theta ratio** remains close to normal (z-score ≈ 0 SD) because both delta and theta increase proportionally.

In contrast to elevated slow-wave ratios, the brain maps show **suppressed activity in the faster frequencies**, particularly within the **alpha and beta bands**:

- The **alpha/beta** and **alpha/high beta** ratios fall within the **0 to –1 SD** range, suggesting mild reductions.
- These areas often appear blue or white on the map, with some regions (e.g., central, temporal, and parietal lobes) maintaining near-normal activity.
- The **beta/high beta** ratio also shows a modest decrease, with estimated z-scores around **–0.5 to –1 SD**.
- Overall, both beta and high beta bands are reduced, but beta appears more suppressed, leading to slightly lower ratio scores.

This general pattern — **increased slow-wave activity and decreased fast-wave activity** — is consistent with findings reported in qEEG studies of MCI and AD [33]. Specifically, elevated **theta/alpha** and **theta/beta** ratios are frequently observed in AD patients and are associated with cognitive slowing, reduced attention, and impaired working memory.

The suppression of alpha and beta activity, especially in posterior and temporal regions, aligns with known neuropathological patterns in Alzheimer's disease [33]. In more advanced stages, frontal slowing may also emerge. These findings reflect reduced cortical arousal, impaired connectivity, and decreased processing efficiency.

Although the patterns shown in Figure 1 support the presence of cognitive impairment, **qEEG alone is not sufficient to diagnose MCI or AD**. These results must be interpreted in conjunction with clinical evaluations, cognitive testing, and neuroimaging for an accurate diagnosis.

The following observations summarize the key patterns evident in the z-scored brain maps:

- **Elevated ratios (Red, +2 to +3 SD):**
  - **Theta/alpha, theta/beta, delta/alpha, delta/beta** → Indicate EEG slowing and potential neurodegeneration
- **Suppressed ratios (Blue, –1 to –2 SD):**
  - **Beta/gamma, alpha/beta, beta/high beta** → Suggest reduced cortical activity or processing
- **Neutral ratios (White, 0 SD):**

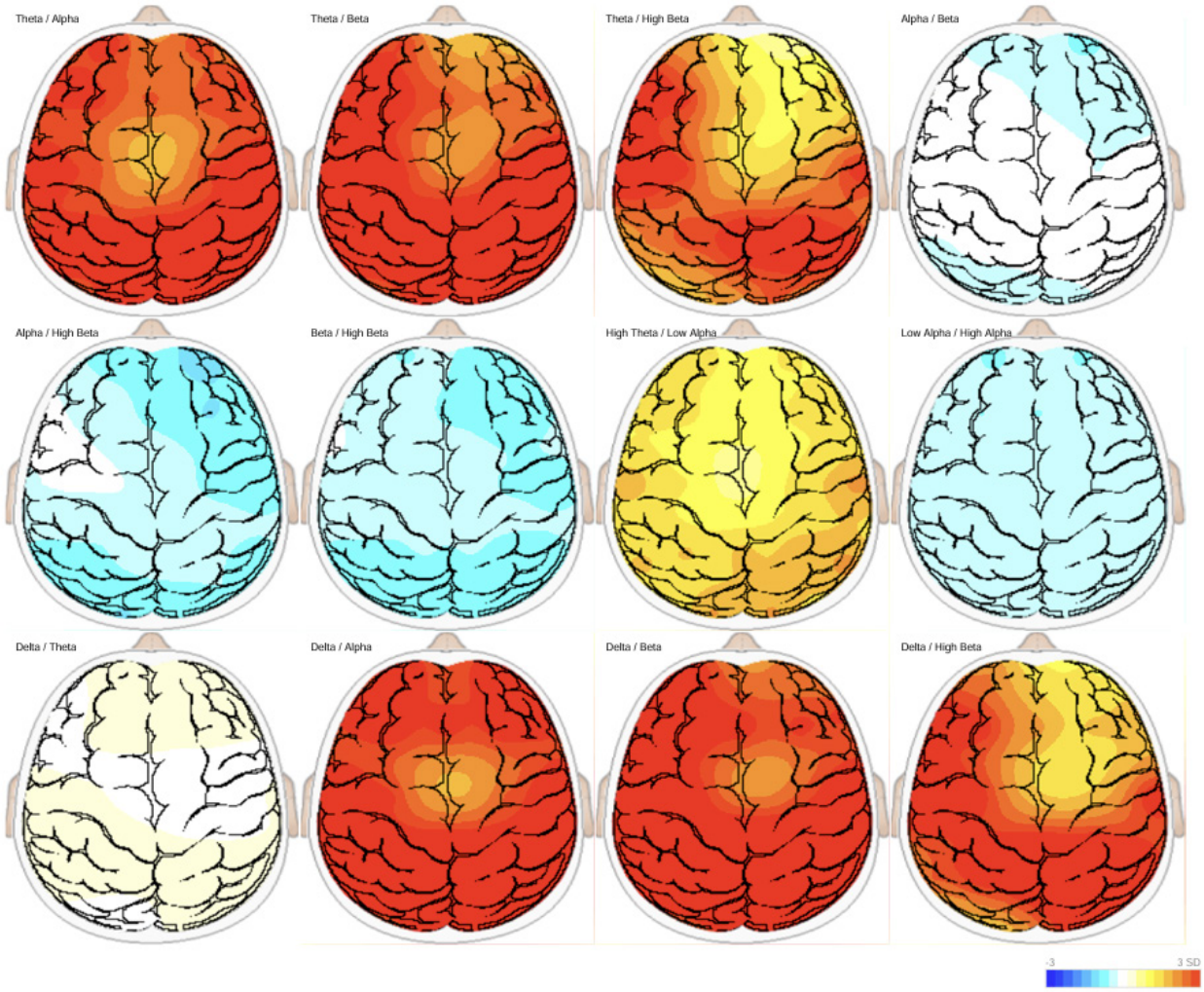

Figure 1: BrainView Z-scored spectral brain maps. A **z-score of 0 SD** indicates activity consistent with a 'healthy' norm. **Positive z-scores** (+1 to +3 SD) reflect **increased activity** in a frequency band. **Negative z-scores** (–1 to –3 SD) indicate **decreased activity**.

o No significant deviation from 'healthy' norms, indicating relatively preserved function in some areas

These brain mapping results can inform **early screening**, guide **treatment planning**, and support **neurofeedback protocols** by identifying regions and frequency bands most affected by cognitive decline.

The increased presence of slow-wave activity (theta and delta) alongside reduced fast-wave activity (alpha and beta) is characteristic of early dementia and is often observed in individuals with AD or advanced MCI [33]. These findings are particularly notable in the **posterior and temporal regions**, which are commonly affected in the early stages of Alzheimer's disease. However, as with all neurophysiological tools, qEEG findings should be integrated with broader clinical data to enhance diagnostic accuracy and ensure appropriate intervention strategies.

B. *Z-Scored Relative Power Brain Map – Frequency Bands*

The z-scored relative power brain map provides a clear visualization of how a client's EEG activity deviates from the normative database established by BrainView. Each scalp map reflects the power of a specific frequency band, expressed in SD (z-score) units relative to 'healthy' population averages. In this context:

· Blue/cyan coloring indicates decreased power (below normal)
· Red/orange coloring indicates increased power (above normal)

The most prominent finding in the client's brain map is a significant increase in delta (2–4 Hz) power, particularly in the frontal regions. This pattern is not typical of 'healthy' adults and is often associated with pathological brain slowing (Figure 2). Delta activity is generally linked to deep sleep, and its presence during awake resting states suggests abnormal neural function.

In addition to delta, there is an increase in theta activity, particularly within the early theta band (theta1, 4–6 Hz). Elevated waking theta, especially in frontal regions, is another classic marker of cognitive decline [33]. While theta is a normal feature during drowsiness, excessive theta during rest while awake is considered a hallmark of MCI and early-stage AD. This increased slow-wave activity reflects impaired information processing and reduced cognitive efficiency.

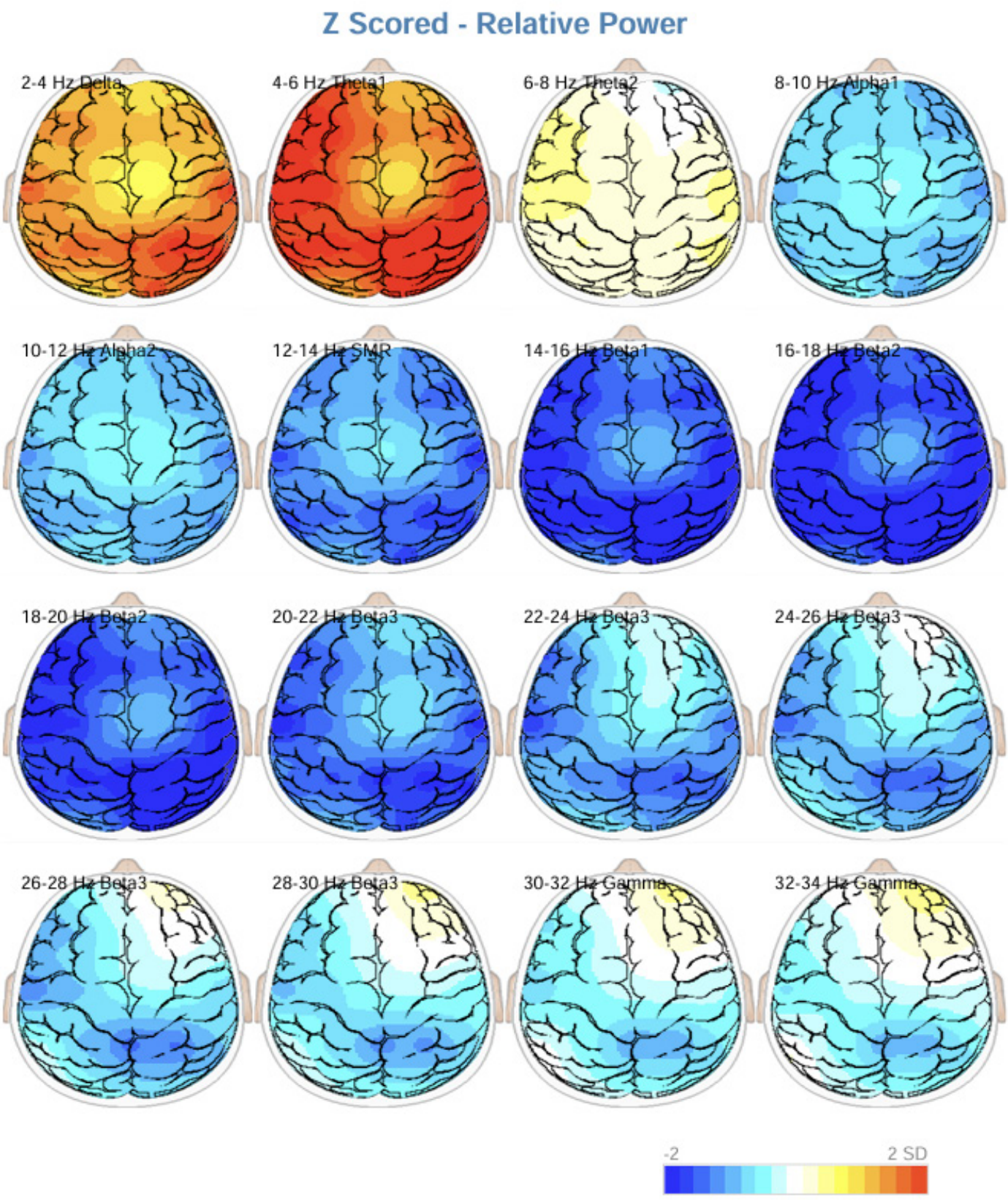

Figure 2: BrainView Z-scored relative power brain maps. Each scalp map reflects the power of a specific frequency band, expressed in SD (z-score) units relative to 'healthy' population averages. Blue/cyan coloring indicates decreased power (below normal). Red/orange coloring indicates increased power (above normal).

Alongside the increase in slow waves, the map reveals reduced power in the alpha band (8–12 Hz), especially in the parietal regions (Figure 2). Alpha rhythms are critical for resting-state coordination, attention, and memory. Suppressed alpha is a common feature of disrupted cognitive function, and is frequently observed in AD and MCI [33]. This reduction reflects impaired connectivity and a breakdown in normal resting-state brain networks.

Beta activity, typically associated with active thinking, focused attention, and motor planning, is also decreased, especially in the lower beta ranges. This decline suggests weakened cognitive engagement and reduced arousal. The combination of elevated delta/theta and reduced beta power is strongly indicative of EEG slowing, a well-established pattern in dementia-related disorders [33].

The Sensorimotor Rhythm (SMR), which falls within the 12–14 Hz range (Figure 2), is a subset of low beta and is typically recorded over the sensorimotor cortex (e.g., C3, Cz, C4). SMR is associated with calm alertness and motor inhibition, where the brain is focused while the body remains physically still. In the client's map, SMR activity is reduced, suggesting impairments in motor control, attention regulation, or functional connectivity — a pattern also consistent with early to mid-stage AD. Low SMR has also been associated with various cognitive and attentional disorders, and is a common target in neurofeedback protocols designed to improve alertness or reduce hyperactivity [74].

Gamma activity appears relatively unchanged in this case. While gamma is linked to higher-order cognitive functions, it is often difficult to interpret reliably in scalp EEG due to its susceptibility to noise and muscle artifacts [75-79]. In some studies, gamma activity in AD patients has been reported as unchanged, reduced, or even elevated, depending on the methodology [80]. Thus, its neutral appearance in this brain map may reflect either a preservation of high-level processing or measurement limitations, rather than a definitive clinical indicator.

The overall pattern observed in Figure 2 is strongly suggestive of advanced MCI or early-stage AD. Key features supporting this interpretation include:

- Excess slow-wave activity in the delta and theta bands
- Suppressed alpha and beta power
- Frontal slowing and posterior hypoactivation

These EEG patterns are not typical of 'healthy' aging and reflect underlying disruptions in large-scale brain networks, particularly the DMN and the fronto-parietal attentional system, both of which are known to degrade in the early stages of AD. The combination of increased delta/theta and reduced beta/alpha activity forms a classic "slowing" pattern in EEG, which aligns with reduced neural efficiency, impaired cognitive control, and loss of network coordination often seen in dementia-related conditions.

The z-scored relative power brain map provides strong neurophysiological evidence of abnormal brain function consistent with MCI or early AD. Specifically, the elevated delta and theta activity, combined with decreased alpha and beta power, suggest impaired attention, memory processing, and cognitive control. Although gamma activity appears unaffected, its interpretation remains limited due to technical constraints.

These findings should be considered in the broader context of clinical evaluation, including neuropsychological testing, functional assessments, and neuroimaging. While EEG slowing is a valuable biomarker, it is not sufficient alone for diagnosis, but rather, serves as a supportive tool in identifying and tracking the progression of cognitive impairment.

C. *Source-Level EEG Findings: sLORETA Analysis*

Standardized Low-Resolution Electromagnetic Tomography (sLORETA) is an advanced EEG source localization method that estimates where in the brain (in three-dimensional space) electrical activity in different frequency bands originates [81]. Unlike traditional EEG scalp topographies, which show surface-level activity, sLORETA projects this activity into the anatomical structure of the brain, enabling visualization of power distribution in specific cortical regions. sLORETA and similar source localization tools are increasingly used in qEEG to identify the likely neural generators of observed activity. This approach is particularly useful for detecting abnormal cortical patterns related to neurodegenerative diseases, such as AD and MCI.

Figure 3 displays a notable increase in theta1 (4–6 Hz) and theta2 (6–8 Hz) power, particularly in the frontal and parietal regions. These areas appear in orange to yellow, indicating elevated theta activity relative to normative databases. This widespread increase in theta power is consistent with cortical slowing, a hallmark of cognitive decline. In particular:

- Excess frontal and parietal theta is frequently observed in early-stage AD and amnestic MCI.
- Theta activity in these regions suggests reduced neural efficiency, as the brain requires more effort to perform cognitive tasks.
- Frontal-midline theta may also reflect executive compensation, a mechanism whereby the brain recruits additional frontal resources to offset deficits in memory or attention, commonly seen in MCI.

These patterns are not typically present in 'healthy' aging and instead reflect early neurodegenerative changes.

The alpha1 band (8–10 Hz) is normally associated with relaxed wakefulness, internal attention, and sensory inhibition. In 'healthy' individuals, alpha activity is most prominent in the posterior cortex, particularly the parietal and occipital lobes, during resting states (especially with eyes closed). However, Figure 3 reveals a widespread reduction in alpha1 power (blue/cyan coloring), particularly in the posterior regions. This posterior alpha hypoactivity is characteristic of:

- Disrupted resting-state networks
- Reduced cortical inhibition and attentional control

· Impaired sensory integration and alertness

This posterior alpha attenuation is very typical in AD and progressed MCI, and reflects functional disconnection within the DMN, a network known to deteriorate early in Alzheimer's pathology.

In Figure 3, SMR activity, associated with calm focus, motor inhibition, and physical stillness with mental alertness, is significantly reduced, particularly in sensorimotor and parietal areas. This suppression is consistent with:

· Impaired motor planning or motor system connectivity
· Reduced functional integrity of sensorimotor networks
· Neurodegeneration associated with early- to mid-stage AD

SMR suppression further supports the presence of both cognitive and sensorimotor slowing, often seen in neurodegenerative conditions [82].

The sLORETA-derived source localization maps provide deeper insight into the client's EEG profile by confirming the presence of abnormal brain activity in anatomically meaningful regions [33]. Specifically, the findings include:

· Elevated theta1 and theta2 activity in frontal and parietal cortices, indicating cortical slowing and possible executive compensation (cortical slowing and compensatory effort).
· Suppressed alpha1 activity in posterior regions, reflecting disrupted resting-state dynamics and reduced cortical inhibition (resting-state network dysfunction).
· Reduced SMR in sensorimotor and parietal regions, suggesting compromised motor planning and connectivity (motor and attentional slowing).

Together, these abnormalities form a pattern that is strongly consistent with early AD or advanced MCI, particularly of the amnestic subtype. These findings are not typical for 'healthy' aging and are well-aligned with known pathophysiological changes in the early phases of AD. Importantly, source-localized qEEG findings

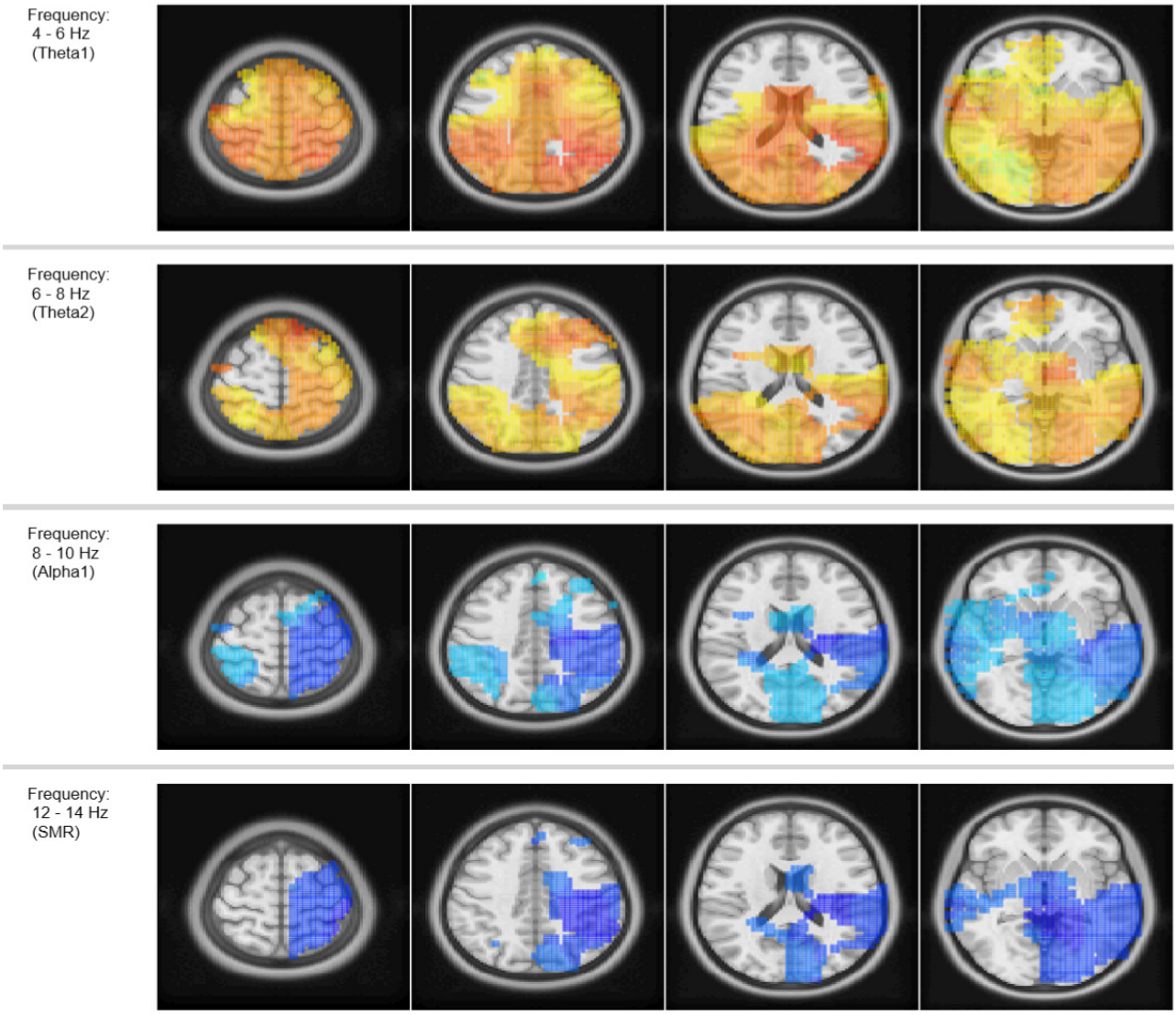

Figure 3: Brain maps of source-level EEG activity (via sLORETA) across different frequency bands. Warm colors (red/yellow) indicates increased power or activation. Cool colors (blue/cyan) indicates decreased power or hypoactivity.

should be integrated with clinical history, neuropsychological testing, and neuroimaging to confirm diagnosis and guide treatment planning.

D. *ERP Analysis*

Figure 4 illustrates averaged ERP waveforms recorded during an oddball paradigm, comparing responses between 'healthy' controls and individuals with AD. The graph displays two traces ─ blue for the control group and red for the AD group ─ plotted across a time window from –0.2 to 1.0 seconds. Voltage amplitudes are represented on the y-axis in microvolts (μV), with reference points provided at +2.31 μV, +0.44 μV, and –1.42 μV.

The ERP components of particular interest in this figure are the P200 (P2) and P300 (P3), both of which are associated with distinct stages of sensory and cognitive processing. The P200, occurring approximately 150–250 milliseconds after stimulus onset, is generally understood to reflect early perceptual processing. In this dataset, the control group shows a pronounced P200 peak, indicative of strong initial sensory engagement. In contrast, the AD group exhibits a reduced P200 response, suggesting diminished or delayed early perceptual processing, a pattern commonly reported in the literature on Alzheimer's and MCI [65].

The P300, typically observed around 300–600 milliseconds post-stimulus, is associated with attention allocation, stimulus evaluation, and working memory updating [83]. In most ERP studies, AD patients tend to show a delayed and attenuated P300 response, reflecting slower cognitive processing and reduced capacity to allocate attentional resources [84-88]. However, the pattern observed in Figure 4 diverges from this expected trend.

Surprisingly, the AD group demonstrates an **earlier and larger** P300 response (approximately 350 ms) compared to the control group's later and smaller P300 (around 400 ms). This atypical finding suggests the possibility of compensatory neural mechanisms at play, particularly in early-stage AD or MCI, where increased cognitive effort or alternative processing strategies may temporarily sustain performance. While this is not the normative pattern seen in mid-to-late stage AD, such results have been reported in some studies under specific task conditions [89]. There is no clear consensus on P300 amplitude, possibly due to methodological differences among the studies [87,89]. Although P300 latency delays are commonly found in individuals with AD, findings in MCI are inconsistent [83]. Some studies report no difference in P300 latency between MCI patients and healthy controls, while others suggest delays in P300 and P3b latency [90-92]. These discrepancies may stem from variations in task design and the heterogeneity of MCI groups.

Interestingly, the control group's weaker P300 response may indicate less effortful engagement with the task or subtle differences in stimulus timing and task demands [89,93]. This observation highlights how ERP outcomes can be influenced not only by disease pathology but also by factors such as task design, sensory modality (e.g., visual vs. auditory), and the specific scalp region used for analysis (e.g., parietal vs. frontal electrodes) [89,94]. The P300 wave is linked to several cognitive processes, including decision-making, memory, orienting, and response selection, particularly during tasks requiring the discrimination of target from non-target stimuli [95-100]. This target selection relies on attention and working memory, as participants must remember and compare stimuli [22,83].

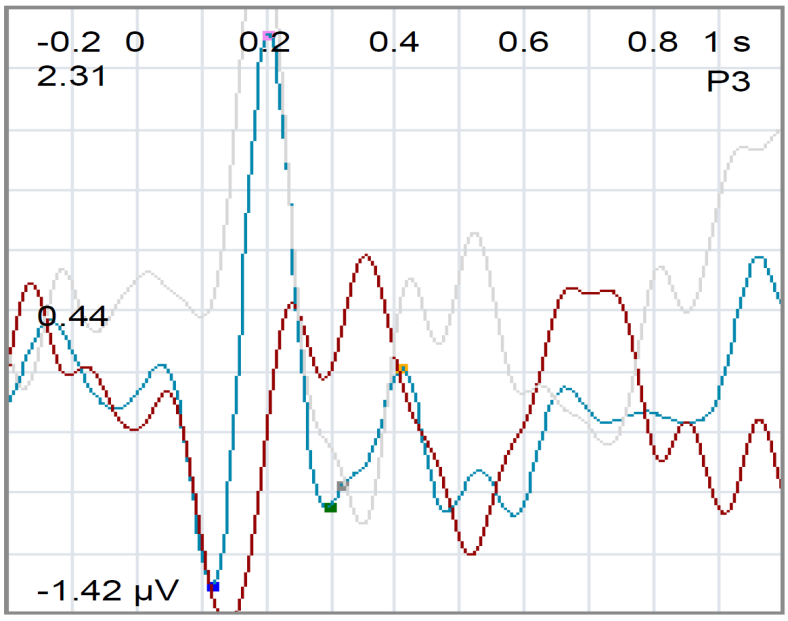

Figure 4: ERP analysis of P200 and P300. The graph displays two traces ─ blue for the control group and red for the AD group ─ plotted across a time window from –0.2 to 1.0 seconds. Voltage amplitudes are represented on the y-axis in microvolts (μV), with reference points provided at +2.31 μV, +0.44 μV, and –1.42 μV.

Although the current findings deviate from typical P300 patterns observed in AD, they are not without precedent. In early stages of cognitive decline, patients may exhibit signs of compensatory activation, leading to earlier or more pronounced ERP responses in certain brain regions [101-103]. Such variability underscores the complexity of using ERP as a diagnostic marker but also points to its potential utility in detecting subtle neurophysiological changes before more overt symptoms emerge. Despite progress in biomarker detection and drug development for AD, its core mechanisms remain unclear [103]. Diagnostic methods have improved through neuroimaging and cerebrospinal fluid biomarkers, yet these often fail to reflect the actual stage of disease progression, as many years may have passed since its onset. This leads to a disconnect between biomarkers and patients' cognitive and functional performance, posing a challenge in clinical practice [103].

As this study serves as a proof of concept for the BrainView system as a potential diagnostic and monitoring tool for MCI and its progression to AD, these preliminary results should be interpreted cautiously. Several factors may contribute to the atypical ERP profiles observed, including the early disease stage of participants, modality-specific task effects, regional brain activity differences, and individual variability within a small sample size.

Further research is essential to validate these findings and refine ERP-based biomarkers for cognitive impairment. Future studies should account for disease stage, task design, and electrode configuration to better understand the mechanisms underlying ERP changes in aging and neurodegeneration.

Discussion

A. QEEG in AD and MCI: Biomarker Potential and Clinical Implications

AD is the most common form of dementia, characterized by progressive deterioration in memory, cognition, and daily functioning. While structural and functional neuroimaging (e.g., MRI, PET) have improved diagnostic accuracy, there remains an urgent need for accessible, cost-effective, and sensitive electrophysiological biomarkers for early detection. EEG and ERP offer high temporal resolution and directly measure cortical activity. In AD, EEG typically shows generalized slowing, with increased delta and theta activity and reduced alpha and beta power, a pattern reflecting cortical dysfunction and disrupted neural communication.

QEEG enhances traditional EEG by applying advanced analyses such as spectral power calculations and source localization. While traditional EEG does not fully meet the 1998 National Institute on Aging biomarker criteria, qEEG shows strong promise as a non-invasive, low-cost tool for detecting early signs of dementia and MCI [104]. BrainView qEEG findings support this promise, revealing:

- Elevated delta and theta power: Indicative of cortical slowing and executive network disruption.
- Suppressed alpha and beta activity: Reflecting impaired resting-state synchrony and cognitive processing.
- Reduced SMR and beta power: Suggesting decreased motor inhibition, increased fatigue, and lower arousal ─ common in neurodegenerative disorders.
- A spatial dissociation pattern of anterior hyperactivity (potentially compensatory) and posterior hypoactivity (degenerative), consistent with early AD and aMCI.

These findings align with previous research, which report EEG slowing, reduced complexity, and weakened connectivity as hallmarks of AD progression [21,42,43,47,105].

Complexity-based EEG features offer additional diagnostic power. For example, Ghassemkhani et al. used fractal dimension and long-range temporal correlations (LRTCs) to distinguish between AD and frontotemporal dementia (FTD) [106]. While both conditions show increased slow-wave power, AD was marked by frontal activity, and FTD by posterior (caudal) changes. These findings highlight the potential of complexity metrics in differentiating dementia subtypes. While complex EEG features are being explored, simple power ratios (e.g., theta/alpha, theta/beta) remain practical and effective diagnostic indicators [21].

B. Source Localization Enhances Spatial Resolution

A key limitation of qEEG is its low spatial resolution, making it difficult to precisely identify the origin of abnormal activity [33]. This is addressed by sLORETA, which localizes cortical sources of EEG signals [81]. In BrainView's sLORETA analysis:

- Theta1 (4–6 Hz) and Theta2 (6–8 Hz) sources were increased in frontal and parietal cortices, possibly reflecting compensatory activation of attention networks.
- Alpha1 (8–10 Hz) and SMR (12–14 Hz) activity were reduced in posterior and sensorimotor regions, indicating disruption of the DMN and motor circuits.

These patterns mirror findings from previous sLORETA/eLORETA studies [33]:

- AD shows reduced posterior alpha activity and increased slow-wave power [40,107,108].
- aMCI patients demonstrate intermediate alpha power and progressive reductions in posterior regions over time.
- EEG source analysis helps differentiate between AD-MCI, DLB-MCI, and healthy aging based on distinct frequency patterns.

C. Clinical Considerations, Limitations, and Integration

While the qEEG patterns observed in AD and MCI are well documented, they are not specific [65,109]. Similar EEG slowing can occur in vascular cognitive impairment, major depression, traumatic brain injury, metabolic disturbances, medication effects, and sleep deprivation or fatigue. Therefore, qEEG must be interpreted in a clinical context, alongside cognitive testing [e.g., Mini-Mental State Examination (MMSE), Montreal Cognitive Assessment (MoCA)], structural and functional imaging, and laboratory and neurological evaluations. To establish qEEG as a primary biomarker in clinical practice, several steps are essential [33]:

- Validation against gold-standard biomarkers (e.g., CSF Aβ/tau,

PET imaging)
- Large, annotated datasets from diverse populations
- Standardization of EEG recording and analysis protocols
- Integration with multimodal tools (e.g., MRI, ERP, AI-based platforms)

Recent efforts emphasize the importance of standardized, multicenter studies to confirm diagnostic reliability and promote broader clinical adoption [110].

QEEG is an emerging, non-invasive, and cost-effective tool for detecting and monitoring AD and related cognitive disorders. By offering real-time, network-level insights into brain function, it complements traditional assessments and may play a central role in personalized dementia care. While it cannot independently diagnose AD or MCI, qEEG provides valuable physiological context that ─ when combined with cognitive and imaging assessments ─ supports early intervention, monitoring, and treatment evaluation. Continued advancements in source localization, data integration, and machine learning will be key to unlocking its full clinical potential.

D. *ERPs in AD: Diagnostic and Research Applications*

ERPs are invaluable in memory research because they provide high temporal resolution, capturing the rapid processes involved in memory encoding and retrieval, both of which are closely linked to synaptic plasticity [111,112]. Later ERP components are particularly sensitive to pathological changes seen in AD, especially in regions such as the medial temporal lobes and association neocortices, which are affected early in the disease [113,114].

Studies using visual stimuli have reported delayed P200 latency in AD patients during pattern reversal or flash paradigms, even when earlier visual components like P100 remain normal [65]. For example, Martinelli, et al. found that delayed P200 latency correlated with visuospatial deficits in AD patients, supporting its use in differentiating AD from other forms of dementia [115]. Similarly, ERP studies using olfactory stimuli, which engage areas vulnerable to early AD pathology, have shown superior sensitivity compared to traditional auditory P300 [85,116]. In one study, olfactory ERP (OERP) components such as P200 and P300 were significantly delayed in AD patients, correlating strongly with disease severity and distinguishing AD from normal aging with up to 92% accuracy [116]. In contrast, studies involving verbal stimuli (spoken or written words) have shown that N100 and P200 components are generally preserved in mild AD, suggesting that early sensory processing in these modalities may be relatively unaffected [117,118].

Longer P200 and N200 latencies have also been reported in AD patients during more demanding cognitive tasks like the two-back working memory task [119]. These mid-latency ERP components may reflect deficits in early attentional and inhibitory control processes, adding to the diagnostic utility of a multi-component ERP approach.

In MCI, several studies have reported abnormalities in N200 and P300 components [120-122]. These include delayed latencies and reduced amplitudes, which may serve as early markers distinguishing MCI from healthy aging [120,122]. However, findings are mixed. For example, Phillips, et al**.**, using the Sternberg working memory task, found no significant differences in P300 or N200 between MCI patients and controls, although reduced P300 amplitude was observed in the AD group [123]. Despite the potential of ERP markers, they are not currently included in the proposed Preclinical AD diagnostic criteria [124]. Nonetheless, their non-invasive, low-cost nature makes them highly promising tools for early detection, particularly in resource-limited settings.

The P300 component, especially P300 latency, has long been recognized as a reliable biomarker for working memory function, which is impaired in AD [125-127]. Elicited during attention-demanding tasks (e.g., oddball paradigms), the P300 waveform is robust and easy to detect, making it suitable for both research and clinical applications [128]. Due to our atypical findings with P300, further research and validation is required to establish BrainView as a reliable diagnostic tool to differentiate AD from other neurological disorders.

In AD, P300 latency tends to increase, while amplitude often decreases as the disease progresses [109]. Although a few studies have reported no amplitude differences between AD patients and healthy controls, the increase in P300 latency is one of the most consistent findings in the ERP literature on AD [94,129,130]. Importantly, no studies have reported shortened P300 latency in AD patients compared to controls, though at least one study found no difference [109,131].

Beyond diagnostics, P300 latency is also sensitive to pharmacological interventions. Studies show that drugs like cholinesterase inhibitors can alter P300 latency and amplitude, indicating their effect on cognitive processing [109]. This makes ERP markers particularly useful for early-phase clinical trials aimed at evaluating drug efficacy. Additionally, prolonged P300 latency has been observed not only in AD but in a range of other conditions including Huntington's disease, transient ischemic attack, intellectual disabilities, ADHD, sleep deprivation, and traumatic brain injury (TBI), further supporting its general utility as a cognitive biomarker [109].

In summary, ERP components**,** especially P300 latency, offer a valuable, non-invasive window into synaptic function and cognitive decline. Their use in detecting and tracking AD and MCI is well supported, and they also hold potential for monitoring treatment effects and predicting therapeutic efficacy. While current diagnostic frameworks have yet to formally include ERP biomarkers, their clinical and research value is increasingly recognized, and ongoing studies are likely to pave the way for their broader adoption.

E. ***Machine Learning Advancements in EEG-Based Diagnosis and Prediction of AD***

Machine learning (ML) is playing an increasingly pivotal role

in enhancing the diagnostic and predictive capabilities of qEEG and other data modalities in AD and MCI. By integrating EEG features, imaging biomarkers, and clinical data with advanced classifiers, ML models are delivering promising results in terms of accuracy, interpretability, and clinical applicability.

The BrainView system demonstrated the diagnostic utility of EEG combined with ML by classifying probable AD versus non-AD 'healthy' controls (N = 83) using the **XGBoost** algorithm with LASSO Logistic Regression. The BrainView model achieved a **sensitivity of 0.88** and **specificity of 0.94**, highlighting the potential of EEG-based features in supporting early diagnosis. These results underscore the effectiveness of tree-based ensemble methods for handling complex, high-dimensional EEG data in neurodegenerative contexts.

Hossain developed an **interpretable ensemble ML model** using data from **2,149 adults aged 60–90**. This **stacked ensemble** combined **Gradient Boosting**, **XGBoost**, and **Logistic Regression** as a meta-learner [132]. The model demonstrated **balanced and robust performance** across AD and non-AD classifications, achieving a **97% AUC**. The meta-learning strategy effectively harnessed the strengths of each base model, enhancing both **predictive power** and **interpretability**, making it suitable for integration into **clinical decision-support systems**.

In a larger longitudinal study, Fernandez-Blazquez and colleagues developed ML models to **predict MCI onset in cognitively healthy older adults** over a three-year period. Using data from **845 individuals aged 65–87**, the most comprehensive XGBoost model, which incorporated demographic, clinical, and cognitive variables, achieved an **accuracy of 86% [71]**. This study reinforces the practicality of non-imaging, ML-based tools for early risk prediction and highlights their cost-effectiveness, especially in large population screenings.

A more advanced approach combined **deep learning and ensemble learning**, utilizing a **fine-tuned VGG19 convolutional neural network** alongside an **XGBoost classifier** to analyze MRI data [133]. This hybrid model achieved an impressive **accuracy of 99.6%**, outperforming traditional classifiers by effectively addressing **class imbalance** and **overfitting [133]**. Key techniques included transfer learning, data augmentation, and ensemble integration. These results support the use of multimodal AI-driven frameworks for high-accuracy AD diagnosis, with future directions focusing on generalizing across diverse populations and integrating additional modalities such as EEG and genetics.

To tackle the challenge of **interpreting ML decisions**, Yi, et al. proposed an interpretable ML framework combining **XGBoost** with **SHAP (SHapley Additive exPlanations) [72]**. The model was designed to classify stages of cognitive decline ─ normal cognition (NC), MCI, and AD ─ while managing class imbalance. It utilized a wide range of features including cognitive scores, imaging biomarkers, and genetic data. Performance results across two major datasets [AD Neuroimaging Initiative (ADNI) and National Alzheimer's Coordinating Center (NACC)]:

- **Accuracy**: 87.6% (ADNI), 80.5% (NACC)
- **AUC**: 0.91 (ADNI), 0.88 (NACC)
- **Sensitivity/Specificity**: >74% and >89%, respectively

This framework not only achieved superior performance compared to traditional classifiers (e.g., Random Forest, AdaBoost, Naive Bayes) but also offered **clinically meaningful interpretability**, allowing clinicians to understand how and why predictions were made.

Jang's study was the first to apply an **XGBoost-based model** using **EEG features alone** for dementia classification [134]. Utilizing **24 EEG features**, the model achieved a **balanced accuracy of 94.12% [134]**. Key differentiators included:

- **Lower alpha/theta (A/T) and alpha-to-baseline ratios** in dementia patients, reflecting reduced attention and working memory.
- Application of **RFECV (Recursive Feature Elimination with Cross-Validation)** to optimize feature selection and model interpretability.
- **Weighted class balancing** to address the challenge of small, imbalanced datasets.

Compared to traditional classifiers like Random Forest, the **XGBoost + RFECV model** delivered superior performance, underscoring the value of tree-based algorithms and EEG biomarkers in early dementia detection.

While these studies, Jang and Hossain, highlight the promising potential of ML in AD diagnosis, several limitations and future research priorities remain [132,134]. These challenges include:

- **Small sample sizes** and **imbalanced datasets** may limit generalizability.
- Most models require **external validation** across larger, more diverse, and longitudinal cohorts.

To broaden the application of ML in AD, future efforts must focus on seamlessly integrating these models into clinical workflows to provide real-time decision support, as proposed by Jang and Hossain [132,134]. A key direction is the fusion of multimodal data, combining EEG, MRI, PET imaging, cognitive assessments, and genetic information, to create a more comprehensive and accurate diagnostic framework. Validation across diverse populations and healthcare settings is essential to ensure that these tools are generalizable and effective in real-world clinical practice. In parallel, the development of federated learning frameworks will allow for secure, privacy-preserving collaboration across institutions, enabling the use of larger, more representative datasets without compromising patient confidentiality. To support widespread clinical adoption, there is also a pressing need for improved interpretability tools that provide clinicians with clear, actionable insights from ML outputs. These advancements, as emphasized by Jang and Hossain, will help translate machine learning from research to routine care in the diagnosis and management of Alzheimer's disease [132,134].

The integration of ML with qEEG, neuroimaging, and clinical data

offers a powerful path toward early, accurate, and interpretable diagnosis of AD and related cognitive disorders. As models become more refined and validated across populations, these AI-driven tools hold the potential to revolutionize dementia care, supporting earlier interventions, personalized treatment strategies, and improved patient outcomes.

Conclusion

This study demonstrates the potential of qEEG and ERPs, in combination with machine learning, as promising tools for the early detection and monitoring of MCI and AD. Through the BrainView system's multi-modal EEG analysis — including z-scored brain maps, sLORETA, and ERP waveforms — consistent neurophysiological patterns were identified that align with established biomarkers of cognitive decline. Specifically, elevated delta and theta activity, coupled with suppressed alpha and beta power, reflect classical EEG slowing observed in early-stage AD. Source-level findings further localized these abnormalities to frontal and parietal cortices, reinforcing the hypothesis of network disruption within the default mode and attentional systems.

ERP analysis revealed attenuated P200 components and an atypically early and amplified P300 response in individuals with suspected early AD or advanced MCI, possibly indicating compensatory neural activation during early disease stages. Although these ERP patterns diverge from canonical AD profiles, they underscore the complexity and individual variability of cognitive decline—highlighting the need for nuanced interpretation based on disease stage and task design.

Machine learning models applied to EEG data demonstrated high sensitivity and specificity in distinguishing between AD and healthy controls. These results validate the diagnostic value of EEG-derived features, especially when supported by interpretable models such as XGBoost with SHAP analysis. Such approaches not only enhance classification accuracy but also offer clinicians greater transparency into model decision-making — an essential step toward integration into routine clinical workflows.

Despite the promising results, EEG-based diagnostics should be viewed as complementary rather than standalone tools. EEG abnormalities can overlap with other neurological and psychiatric conditions, necessitating comprehensive evaluation alongside cognitive testing, neuroimaging, and laboratory assessments. The interpretive power of EEG is further strengthened when integrated with multimodal data and validated in diverse populations.

In summary, qEEG and ERP analysis — augmented by source localization and machine learning — offer valuable insights into the functional neurodynamics of MCI and early AD. As standardization and validation efforts continue, these non-invasive, cost-effective techniques have the potential to support earlier diagnosis, guide individualized interventions, and monitor disease progression with greater precision.

References

1. Lynch, C. World Alzheimer Report 2019: Attitudes to dementia a global survey Public health: Engaging people in ADRD research. Alzheimers Dement. 2020; 16: e038255.
2. Tautan AM, Casula EP, Pellicciari MC, et al. TMS-EEG perturbation biomarkers for Alzheimer's disease patients classification. Sci Rep. 2023; 13: 7667.
3. Brookmeyer R, Evans DA, Hebert L, et al. National estimates of the prevalence of Alzheimer's disease in the United States. Alzheimers Dement. 2011; 7: 61-73.
4. Fratiglioni L, Grut M, Forsell Y, et al. Prevalence of Alzheimer's disease and other dementias in an elderly urban population: Relationship with age, sex, and education. Neurology. 1991; 41: 1886-1892.
5. Long S, Benoist C, Weidner W. World Alzheimer Report 2023: Reducing dementia risk: Never too early never too late. Alzheimer's Disease International. 2023.
6. Prince M, Wimo A, Guerchet M. World Alzheimer Report 2015: The global impact of dementia. Alzheimer's Disease International. 2015.
7. The global impact of dementia 2013-2050. Alzheimer's Disease International. 2013.
8. Rajan KB, Weuve J, Barnes LL, et al. Population estimate of people with clinical Alzheimer's disease and mild cognitive impairment in the United States (2020–2060). Alzheimers Dement. 2020; 17: 1966-1975.
9. Knopman DS, Petersen RC, Jack CR Jr. A brief history of "Alzheimer disease": Multiple meanings separated by a common name. Neurology. 2019; 92: 1053-1059.
10. Kazim SF, Seo JH, Bianchi R, et al. Neuronal network excitability in Alzheimer's disease: The puzzle of similar versus divergent roles of amyloid â and tau. eNeuro. 2021; 8: ENEURO.0418-20.2020.
11. Dunn AR, Kaczorowski CC. Regulation of intrinsic excitability: Roles for learning and memory, aging and Alzheimer's disease, and genetic diversity. Neurobiol Learn Mem. 2019; 164: 107069.
12. Haberman RP, Koh MT, Gallagher M. Heightened cortical excitability in aged rodents with memory impairment. Neurobiol Aging. 2017; 54: 144-151.
13. Benwell CSY, Davila Pérez P, Fried PJ, et al. EEG spectral power abnormalities and their relationship with cognitive dysfunction in patients with Alzheimer's disease and type 2 diabetes. Neurobiol Aging. 2020; 85: 83-95.
14. Gaubert S, Raimondo F, Houot M, et al. EEG evidence of compensatory mechanisms in preclinical Alzheimer's disease. Brain. 2019; 142: 2096-2112.
15. Musaeus CS, Engedal K, Høgh P, et al. Oscillatory connectivity as a diagnostic marker of dementia due to Alzheimer's disease. Clin Neurophysiol. 2019; 130: 1889-1899.
16. Puttaert D, Coquelet N, Wens V, et al. Alterations in resting-state network dynamics along the Alzheimer's disease continuum. Sci Rep. 2020; 10: 21990.

17. Jun H, Bramian A, Soma S, et al. Disrupted place cell remapping and impaired grid cells in a knockin model of Alzheimer's disease. Neuron. 2020; 107: 1095-1112.e6.
18. Sciaccaluga M, Megaro A, Bellomo G, et al. An unbalanced synaptic transmission: Cause or consequence of the amyloid oligomers neurotoxicity?. Int J Mol Sci. 2021; 22: 5991.
19. Cummings J, Zhou Y, Lee G, et al. Alzheimer's disease drug development pipeline: 2023. Alzheimers Dement (N Y). 2023; 9: e12385.
20. Liu JZ, Smotrys MA, Robinson SD, et al. Quantitative EEG evidence of cognitive restoration in Alzheimer's disease following biophoton generator therapy. J Neurol Res Rev Rep. 2025; 7: 1-11.
21. Ding Y, Chu Y, Liu M, et al. Fully automated discrimination of Alzheimer's disease using resting-state electroencephalography signals. Quant Imaging Med Surg. 2022; 12: 1063-1078.
22. Polich J. Updating P300: An integrative theory of P3a and P3b. Clin Neurophysiol. 2007; 118: 2128-2148.
23. Simic G, Babic M, Borovecki F, et al. Early failure of the default-mode network and the pathogenesis of Alzheimer's disease. CNS Neurosci Ther. 2014; 20: 692-698.
24. Anderson ND. State of the science on mild cognitive impairment (MCI). CNS Spectr. 2019; 24: 78-87.
25. Perrin RJ, Fagan AM, Holtzman DM. Multimodal techniques for diagnosis and prognosis of Alzheimer's disease. Nature. 2009; 461: 916-922.
26. Craig Schapiro R, Kuhn M, Xiong C, et al. Multiplexed immunoassay panel identifies novel CSF biomarkers for Alzheimer's disease diagnosis and prognosis. PLoS One. 2011; 6: e18850.
27. Kim S, Lee Y, Jeon CY, et al. Quantitative magnetic susceptibility assessed by 7T magnetic resonance imaging in Alzheimer's disease caused by streptozotocin administration. Quant Imaging Med Surg. 2020; 10: 789-797.
28. Appel J, Potter E, Shen Q, et al. A comparative analysis of structural brain MRI in the diagnosis of Alzheimer's disease. Behav Neurol. 2009; 21: 13-19.
29. Marcus C, Mena E, Subramaniam RM. Brain PET in the diagnosis of Alzheimer's disease. Clin Nucl Med. 2014; 39: e413-e422
30. Yang F, Jiang J, Alberts I, et al. Combining PET with MRI to improve predictions of progression from mild cognitive impairment to Alzheimer's disease: An exploratory radiomic analysis study. Ann Transl Med. 2022; 10: 513.
31. Buzsaki G, Anastassiou CA, Koch C. The origin of extracellular fields and currents—EEG, ECoG, LFP and spikes. Nat Rev Neurosci. 2012; 13: 407-420.
32. Buzsaki G. Rhythms of the brain. Oxford University Press. 2006.
33. Yuan Y, Zhao Y. The role of quantitative EEG biomarkers in Alzheimer's disease and mild cognitive impairment: Applications and insights. Front Aging Neurosci. 2025; 17: 1522552.
34. Van der Hiele K, Vein AA, Reijntjes RHAM, et al. EEG correlates in the spectrum of cognitive decline. Clin Neurophysiol. 2007; 118: 1931-1939.
35. Pritchard WS, Duke DW, Coburn KL, et al. EEG-based neural-net predictive classification of Alzheimer's disease versus control subjects is augmented by non-linear EEG measures. Electroencephalogr Clin Neurophysiol. 1994; 91: 118-130.
36. Suk HI, Lee SW, Shen D. Latent feature representation with stacked auto-encoder for AD/MCI diagnosis. Brain Struct Funct. 2015; 220: 841-859.
37. Adler G, Brassen S, Jajcevic A. EEG coherence in Alzheimer's dementia. J Neural Transm (Vienna). 2003; 110: 1051-1058.
38. Huang C, Wahlund L, Dierks T, et al. Discrimination of Alzheimer's disease and mild cognitive impairment by equivalent EEG sources: A cross-sectional and longitudinal study. Clin Neurophysiol. 2000; 111: 1961-1967.
39. Bennys K, Rondouin G, Vergnes C, et al. Diagnostic value of quantitative EEG in Alzheimer's disease. Neurophysiol Clin. 2001; 31: 153-160.
40. Kim JS, Lee SH, Park G, et al. Clinical implications of quantitative electroencephalography and current source density in patients with Alzheimer's disease. Brain Topogr. 2012; 25: 461-474.
41. Cassani R, Estarellas M, San Martin R, et al. Systematic review on resting-state EEG for Alzheimer's disease diagnosis and progression assessment. Dis Markers. 2018; 2018: 5174815.
42. Koenig T, Prichep L, Dierks T, et al. Decreased EEG synchronization in Alzheimer's disease and mild cognitive impairment. Neurobiol Aging. 2005; 26: 165-171.
43. Dauwels J, Srinivasan K, Reddy MR, et al. Slowing and loss of complexity in Alzheimer's EEG: Two sides of the same coin?. Int J Alzheimers Dis. 2011; 2011: 539621.
44. Jeong J. EEG dynamics in patients with Alzheimer's disease. Clin Neurophysiol. 2004; 115: 1490-1505.
45. Dauwels J, Vialatte F, Cichocki A. Diagnosis of Alzheimer's disease from EEG signals: Where are we standing?. Curr Alzheimer Res. 2010; 7: 487-505.
46. Dauwels J, Vialatte FB, Cichocki A. On the Early Diagnosis of Alzheimer's Disease from EEG Signals: A Mini-Review. Advances in Cognitive Neurodynamics. 2010; 709-716.
47. Babiloni C, Lizio R, Marzano N, et al. Brain neural synchronization and functional coupling in Alzheimer's disease as revealed by resting state EEG rhythms. Int J Psychophysiol. 2016; 103: 88-102.
48. Besthorn C, Förstl H, Geiger Kabisch C, et al. EEG coherence in Alzheimer disease. Electroencephalogr Clin Neurophysiol. 1994; 90: 242-245.
49. Safi MS, Safi SMM. Early detection of Alzheimer's disease from EEG signals using Hjorth parameters. Biomedical Signal Processing and Control. 2021; 65: 102338.
50. AlSharabi K, Bin Salamah Y, Aljalal M, et al. EEG-based clinical decision support system for Alzheimer's disorders

diagnosis using EMD and deep learning techniques. Front Hum Neurosci. 2023; 17: 1190203.

51. Jack CR Jr, Knopman DS, Jagust WJ, et al. Hypothetical model of dynamic biomarkers of the Alzheimer's pathological cascade. Lancet Neurol. 2010; 9: 119-128.
52. Beach TG, Monsell SE, Phillips LE, et al. Accuracy of the clinical diagnosis of Alzheimer disease at National Institute on Aging Alzheimer Disease Centers, 2005–2010. J Neuropathol Exp Neurol. 2012; 71: 266-273.
53. Duncan Johnson CC, Donchin E. The P300 component of the event-related brain potential as an index of information processing. Biol Psychol. 1982; 14: 1-52.
54. Kutas M, McCarthy G, Donchin E. Augmenting mental chronometry: The P300 as a measure of stimulus evaluation time. Science. 1977; 197: 792-795.
55. Polich J, Corey Bloom J. Alzheimer's disease and P300: Review and evaluation of task and modality. Curr Alzheimer Res. 2005; 2: 515-525.
56. Fjell AM, Walhovd KB. P300 and neuropsychological tests as measures of aging: scalp topography and cognitive changes. Brain Topogr. 2001; 14: 25-40.
57. Baudic S, Dalla Barba G, Thibaudet MC, et al. Executive function deficits in early Alzheimer's disease and their relations with episodic memory. Arch Clin Neuropsychol. 2006; 21: 15-21.
58. Caselli RJ, Dueck AC, Locke DEC, et al. Longitudinal modeling of frontal cognition in APOE å4 homozygotes heterozygotes and noncarriers. Neurology. 2011; 76: 1383-1388.
59. Lim YY, Maruff P, Pietrzak RH, et al. Effect of amyloid on memory and non-memory decline from preclinical to clinical Alzheimer's disease. Brain. 2014; 137: 221-231.
60. Cecchi M, Moore DK, Sadowsky CH, et al. A clinical trial to validate event related potential markers of Alzheimer's disease in outpatient settings. Alzheimers Dement (Amst). 2015; 1: 387-394.
61. Bennys K, Rondouin G, Benattar E, et al. Can event-related potential predict the progression of mild cognitive impairment?. J Clin Neurophysiol. 2011; 28: 625-632
62. Olichney JM, Taylor JR, Gatherwright J, et al. Patients with MCI and N400 or P600 abnormalities are at very high risk for conversion to dementia. Neurology. 2008; 70: 1763-1770.
63. Jackson CE, Snyder PJ. Electroencephalography and event-related potentials as biomarkers of mild cognitive impairment and mild Alzheimer's disease. Alzheimers Dement. 2008; 4: S137-S143.
64. Vecchio F, Määttä S. The use of auditory event-related potentials in Alzheimer's disease diagnosis. Int J Alzheimers Dis. 2011; 2011: 653173.
65. Olichney JM, Yang JC, Taylor J, et al. Cognitive event-related potentials: biomarkers of synaptic dysfunction across the stages of Alzheimer's disease. J Alzheimers Dis. 2011; 26: 215-228.
66. Quiroz YT, Ally BA, Celone K, et al. Event-related potential markers of brain changes in preclinical familial Alzheimer disease. Neurology. 2011; 77: 469-475.
67. Young ATL, Danev S, Lakey JRT. Construction and validation of a new BrainView qEEG discriminant database. Acta Scientific Neurology. 2024; 7: 25-51.
68. Knyazev GG. Cross-frequency coupling of brain oscillations: An impact of state anxiety. Int J Psychophysiol. 2011; 80: 236-245.
69. Andersen SB, Moore RA, Venables L, et al. Electrophysiological correlates of anxious rumination. Int J Psychophysiol. 2009; 71: 156-169.
70. Rapp PE, Keyser DO, Albano A, et al. Traumatic brain injury detection using electrophysiological methods. Front Hum Neurosci. 2015; 9: 11.
71. Fernandez Blazquez MA, Ruiz-Sanchez de Leon JM, Sanz Blasco R, et al. XGBoost models based on non-imaging features for the prediction of mild cognitive impairment in older adults. Sci Rep. 2025; 15: 29732.
72. Yi F, Yang H, Chen D, et al. XGBoost-SHAP-based interpretable diagnostic framework for Alzheimer's disease. BMC Med Inform Decis Mak. 2023; 23: 137.
73. Pascual-Marqui RD. Standardized low-resolution brain electromagnetic tomography (sLORETA): Technical details. Methods Find Exp Clin Pharmacol. 2002; 24: 5-12.
74. Marlats F, Bao G, Chevallier S, et al. SMR/Theta neurofeedback training improves cognitive performance and EEG activity in elderly with mild cognitive impairment: A pilot study. Front Aging Neurosci. 2020; 12: 147.
75. Liberati G, Klöcker A, Algoet M, et al. Gamma-band oscillations preferential for nociception can be recorded in the human insula. Cereb Cortex. 2018; 28: 3650-3664.
76. Chouchou F, Perchet C, Garcia Larrea L. EEG changes reflecting pain: Is alpha suppression better than gamma enhancement?. Neurophysiol Clin. 2021; 51: 209-218.
77. Liberati G, Mulders D, Algoet M, et al. Insular responses to transient painful and non-painful thermal and mechanical spinothalamic stimuli recorded using intracerebral EEG. Sci Rep. 2020; 10: 22319.
78. Mussigmann T, Lefaucheur JP, Mc Gonigal A. Gamma-band activities in the context of pain: A signal from brain or muscle?. Neurophysiol Clin. 2021; 51: 287-289.
79. Liberati G, Algoet M, Klöcker A, et al. Habituation of phase-locked local field potentials and gamma-band oscillations recorded from the human insula. Sci Rep. 2018; 8: 8265.
80. Shu IW, Lin Y, Granholm EL, et al. A focused review of gamma neuromodulation as a therapeutic target in Alzheimer's spectrum disorders. J Psychiatr Brain Sci. 2024; 9: e240001.
81. Pascual Marqui RD, Michel CM, Lehmann D. Low resolution electromagnetic tomography: A new method for localizing electrical activity in the brain. International Journal of Psychophysiology. 1994; 18: 49-65.

82. Marlats F, Djabelkhir Jemmi L, Azabou E, et al. Comparison of effects between SMR/delta-ratio and beta1/theta-ratio neurofeedback training for older adults with mild cognitive impairment: A protocol for a randomized controlled trial. Trials. 2019; 20: 88.

83. Demirayak P, Kýyý Ý, Ýþbitiren YÖ, et al. Cognitive load associates prolonged P300 latency during target stimulus processing in individuals with mild cognitive impairment. Sci Rep. 2023; 13: 15956.

84. Patterson JV, Michalewski HJ, Starr A. Latency variability of the components of auditory event-related potentials to infrequent stimuli in aging, Alzheimer-type dementia, and depression. Electroencephalogr Clin Neurophysiol. 1988; 71: 450-460.

85. Polich J, Ladish C, Bloom FE. P300 assessment of early Alzheimer's disease. Electroencephalogr Clin Neurophysiol. 1990; 77: 179-189.

86. Polich J. Normal variation of P300 from auditory stimuli. Electroencephalogr Clin Neurophysiol. 1986; 65: 236-240.

87. Golob EJ, Starr A. Effects of stimulus sequence on event-related potentials and reaction time during target detection in Alzheimer's disease. Clin Neurophysiol. 2000; 111: 1438-1449.

88. Ball SS, Marsh JT, Schubarth G, et al. Longitudinal P300 latency changes in Alzheimer's disease. J Gerontol. 1989; 44: M195-M200.

89. Pedroso RV, Fraga FJ, Corazza DI, et al. P300 latency and amplitude in Alzheimer's disease: A systematic review. Braz J Otorhinolaryngol. 2012; 78: 126-132.

90. Morrison C, Rabipour S, Knoefel F, et al. Auditory event-related potentials in mild cognitive impairment and Alzheimer's disease. Curr Alzheimer Res. 2018; 15: 702-715.

91. Morrison C, Rabipour S, Taler V, et al. Visual event-related potentials in mild cognitive impairment and Alzheimer's disease: A literature review. Curr Alzheimer Res. 2019; 16: 67-89.

92. Paitel ER, Samii MR, Nielson KA. A systematic review of cognitive event-related potentials in mild cognitive impairment and Alzheimer's disease. Behav Brain Res. 2021; 396: 112904.

93. Ribeiro CPHA, Munhoz MSL. O P300 auditivo em jovens e adultos saudáveis com uma nova proposta de resposta: levantar a mão / Cognitive potential (P300) in healthy young and adults using a new strategy: raising hands. Acta AWHO. 999; 18: 32-37.

94. Lai CL, Lin RT, Liou LM, et al. The role of event-related potentials in cognitive decline in Alzheimer's disease. Clin Neurophysiol. 2010; 121: 194-199.

95. Steiner GZ, Barry RJ, Gonsalvez CJ. Can working memory predict target-to-target interval effects in the P300?. Int J Psychophysiol. 2013; 89: 399-408.

96. Scharinger C, Soutschek A, Schubert T, et al. Comparison of the working memory load in N-back and working memory span tasks by means of EEG frequency band power and P300 amplitude. Front Hum Neurosci. 2017; 11: 6.

97. Oliva C, Changoluisa V, Rodríguez FB, et al. Precise temporal P300 detection in brain computer interface EEG signals using a long-short term memory. Springer International Publishing. 2021; 12894: 457-468.

98. Basar Eroglu C, Basar E, Demiralp T, et al. P300-response: Possible psychophysiological correlates in delta and theta frequency channels. A review. Int J Psychophysiol. 1992; 13: 161-179.

99. Dallmer Zerbe I, Popp F, Lam AP, et al. Transcranial alternating current stimulation (tACS) as a tool to modulate P300 amplitude in attention deficit hyperactivity disorder (ADHD): Preliminary findings. Brain Topogr. 2020; 33: 191-207.

100. Marchetti M, Piccione F, Silvoni S, et al. Exogenous and endogenous orienting of visuospatial attention in P300-guided brain computer interfaces: A pilot study on healthy participants. Clinical Neurophysiology. 2012; 123: 774-779.

101. Bobkova N, Vorobyov V. The brain compensatory mechanisms and Alzheimer's disease progression: A new protective strategy. Neural Regen Res. 2015; 10: 696-697.

102. Kanishka, Jha SK. Compensatory cognition in neurological diseases and aging: A review of animal and human studies. Aging Brain. 2022; 3: 100061.

103. Torrealba E, Aguilar Zerpa N, Garcia Morales P, et al. Compensatory mechanisms in early Alzheimer's disease and clinical setting: The need for novel neuropsychological strategies. J Alzheimers Dis Rep. 2023; 7: 513-525.

104. Abo Hagar A, Ashour Y, Abd El Razek R, et al. Quantitative electroencephalographic changes and hippocampal atrophy in diabetic patients with mild cognitive impairment in Ismailia region. Egypt J Neurol Psychiatr Neurosurg. 2018; 54: 15.

105. Hogan MJ, Swanwick GR, Kaiser J, et al. Memory-related EEG power and coherence reductions in mild Alzheimer's disease. Int J Psychophysiol. 2003; 49: 147-163.

106. Ghassemkhani K, Saroka KS, Dotta BT. Evaluating EEG complexity and spectral signatures in Alzheimer's disease and frontotemporal dementia: Evidence for rostrocaudal asymmetry. NPJ Aging. 2025; 11: 50.

107. Babiloni C, Cassetta E, Binetti G, et al. Resting EEG sources correlate with attentional span in mild cognitive impairment and Alzheimer's disease. Eur J Neurosci. 2007; 25: 3742-3757.

108. Babiloni C, Lizio R, Del Percio C, et al. Cortical sources of resting state EEG rhythms are sensitive to the progression of early stage Alzheimer's disease. J Alzheimers Dis. 2013; 34: 1015-1035.

109. Olichney J, Xia J, Church KJ, et al. Predictive power of cognitive biomarkers in neurodegenerative disease drug development: Utility of the P300 event-related potential. Neural Plast. 2022; 2022: 2104880.

110. Babiloni C, Arakaki X, Azami H, et al. Measures of resting state EEG rhythms for clinical trials in Alzheimer's disease: Recommendations of an expert panel. Alzheimers Dement. 2021; 17: 1528-1553.

111. Schack B, Weiss S. Quantification of phase synchronization phenomena and their importance for verbal memory processes. Biol Cybern. 2005; 92: 275-287.

112. Ang CW, Carlson GC, Coulter DA. Hippocampal CA1 circuitry dynamically gates direct cortical inputs preferentially at theta frequencies. J Neurosci. 2005; 25: 9567-9580.

113. Braak H, Braak E. Neuropathological stageing of Alzheimer-related changes. Acta Neuropathol. 1991; 82: 239-259.

114. Katada E, Sato K, Ojika K, et al. Cognitive event-related potentials: Useful clinical information in Alzheimer's disease. Curr Alzheimer Res. 2004; 1: 63-69.

115. Martinelli V, Locatelli T, Comi G, et al. Pattern visual evoked potential mapping in Alzheimer's disease: Correlations with visuospatial impairment. Dementia. 1996; 7: 63-68.

116. Morgan CD, Murphy C. Olfactory event-related potentials in Alzheimer's disease. J Int Neuropsychol Soc. 2002; 8: 753-763.

117. Revonsuo A, Portin R, Juottonen K, et al. Semantic processing of spoken words in Alzheimer's disease: An electrophysiological study. J Cogn Neurosci. 1998; 10: 408-420.

118. Ford JM, Askari N, Mathalon DH, et al. Event-related brain potential evidence of spared knowledge in Alzheimer's disease. Psychol Aging. 2001; 16: 161-176.

119. Missonnier P, Deiber MP, Gold G, et al. Working memory load-related electroencephalographic parameters can differentiate progressive from stable mild cognitive impairment. Neuroscience. 2007; 150: 346-356.

120. Papaliagkas VT, Kimiskidis VK, Tsolaki MN, et al. Cognitive event-related potentials: Longitudinal changes in mild cognitive impairment. Clin Neurophysiol. 2011; 122: 1322-1326.

121. Papaliagkas V, Kimiskidis V, Tsolaki M, et al. Usefulness of event-related potentials in the assessment of mild cognitive impairment. BMC Neurosci. 2008; 9: 107.

122. Bennys K, Portet F, Touchon J, et al. Diagnostic value of event-related evoked potentials N200 and P300 subcomponents in early diagnosis of Alzheimer's disease and mild cognitive impairment. J Clin Neurophysiol. 2007; 24: 405-412.

123. Phillips NA, Chertkow H, Leblanc MM, et al. Functional and anatomical memory indices in patients with or at risk for Alzheimer's disease. J Int Neuropsychol Soc. 2004; 10: 200-210.

124. Sperling RA, Aisen PS, Beckett LA., et al. Toward defining the preclinical stages of Alzheimer's disease: Recommendations from the National Institute on Aging-Alzheimer's Association workgroups on diagnostic guidelines for Alzheimer's disease. Alzheimers Dement. 2011; 7: 280-292.

125. Raskin J, Cummings J, Hardy J, et al. Neurobiology of Alzheimer's disease: Integrated molecular, physiological, anatomical, biomarker, and cognitive dimensions. Current Alzheimer Research. 2015; 12: 712-722.

126. Jackson J, Jambrina E, Li J, et al. Targeting the synapse in Alzheimer's disease. Front Neurosci. 2019; 13: 735.

127. Selkoe DJ. Alzheimer's disease is a synaptic failure. Science. 2002; 298: 789-791.

128. Goodin DS, Squires KC, Starr A. Long latency event-related components of the auditory evoked potential in dementia. Brain. 1978; 101: 635-648.

129. Hedges D, Janis R, Mickelson S, et al. P300 amplitude in Alzheimer's disease: A meta-analysis and meta-regression. Clin EEG Neurosci. 2016; 47: 48-55.

130. Caravaglios G, Costanzo E, Palermo F, et al. Decreased amplitude of auditory event-related delta responses in Alzheimer's disease. Int J Psychophysiol. 2008; 70: 23-32.

131. Lee MS, Lee SH, Moon EO, Et al. Neuropsychological correlates of the P300 in patients with Alzheimer's disease. Prog Neuropsychopharmacol Biol Psychiatry. 2013; 40: 62-69.

132. Hossain MK, Ashraf A, Islam MM, et al. Optimizing Alzheimer's disease prediction through ensemble learning and feature interpretability with SHAP-based feature analysis. Alzheimers Dement (Amst). 2025; 17: e70162.

133. Boudi A, He J, Abd El Kader I, et al. Advancing Alzheimer's disease diagnosis using VGG19 and XGBoost: A neuroimaging-based method. Curr Alzheimer Res. 2025.

134. Jang KI, Kim YI, Ju HJ, et al. Dementia classification using two-channel electroencephalography features. Sci Rep. 2025; 15: 11513.

© 2025 Annie TL Young, et al. This article is distributed under the terms of the Creative Commons Attribution 4.0 International License